

Spin-forbidden transitions in the molecular nanomagnet V₁₅Maren Gysler,¹ Christoph Schlegel,² Tamoghna Mitra,³ Achim Müller,³ Bernt Krebs,⁴ and Joris van Slageren^{1,*}¹*Institut für Physikalische Chemie, Universität Stuttgart, Pfaffenwaldring 55, 70569 Stuttgart, Germany*²*Physikalisches Institut, Universität Stuttgart, Pfaffenwaldring 57, 70569 Stuttgart, Germany*³*Fakultät für Chemie, Universität Bielefeld, 33501 Bielefeld, Germany*⁴*Institut für Anorganische und Analytische Chemie, University Münster, Corrensstrasse 36, 48149 Münster, Germany*

(Received 25 April 2014; revised manuscript received 17 September 2014; published 3 October 2014)

We performed electron spin-resonance measurements on single crystals of the molecular nanomagnet V₁₅ using a novel broadband spectrometer, both in parallel and in perpendicular modes, we see ($B_1 \parallel B_0, B_1 \perp B_0$). Measurements were carried out in proximity of the spin level crossing at $B_0 = 2.75$ T. We observed spin-forbidden transitions from the $S = 1/2$ zero-field ground state to the $S = 3/2$ excited state in parallel mode spectra. Spin-forbidden transitions are employed for switching of coherent interactions between qubits in recent quantum simulator proposals. Our theoretical investigations showed that the mixing of spin states can result from either an antisymmetric exchange interaction or a combination of static distortion and hyperfine interaction.

DOI: [10.1103/PhysRevB.90.144405](https://doi.org/10.1103/PhysRevB.90.144405)

PACS number(s): 75.50.Xx, 75.10.Dg, 75.10.Jm, 76.30.—v

I. INTRODUCTION

Molecular nanomagnets (MNM) are promising candidates for application as qubits in quantum information processing (QIP) [1–3]. A crucial prerequisite for this purpose is a sufficient quantum coherence time, which is the time available for a quantum computation. This time must be longer than the duration of all coherent manipulations of the qubits [4–6]. Trinuclear clusters are especially suitable as the exchange interaction of triangular MNMs can be controlled by both magnetic and electric fields [7,8] where the electric field couples to the chirality of the spin states of the system. In addition, they can exhibit long quantum coherence times [6,9,10]. Performing quantum computations often requires the possibility of switching the qubit coupling during gating operations as well as addressing individual qubits [2,3]. Switching interactions between MNMs can be implemented by the excitation of transitions to specific higher-lying spin states [1] by means of microwave magnetic fields. These excitations correspond to formally forbidden electron spin-resonance (ESR) transitions. To allow such transitions, mixing between spin states is required [7,11,12]. Mechanisms which allow intermultiplet transitions are antisymmetric and anisotropic exchange interactions [13], hyperfine interactions [14], as well as single-ion zero-field splitting [12]. In the above context, the MNM $K_6[V_{15}As_6O_{42}(H_2O)]_8H_2O$ [15,16] (abbreviated V₁₅) is an attractive candidate. It was shown that long-lived coherent superpositions of spin states can be generated within both the ground state ($S = 1/2$) and the first excited state ($S = 3/2$) [6,17,18]. Coherent superposition states that involve both the $S = 1/2$ and the $S = 3/2$ states at the same time. Therefore, demonstrating mixing of spin states within V₁₅ is a step towards achieving coherent superpositions of different total spin multiplets. The MNM V₁₅ consists of 15 antiferromagnetically coupled V⁴⁺ ions, arranged in a quasispherical layered structure formed by a triangle sandwiched between two hexagons [19,20] possessing overall D_3 symmetry. At low temperatures, the spins within each hexagon are coupled

to a total singlet spin $S = 0$ [21]. Therefore, the low-lying energy levels of V₁₅ can be described considering the three spins of the triangle [22–24]. The ground state of this frustrated triangle system consists of two $S = 1/2$ Kramers doublets with the excited $S = 3/2$ quartet state separated from the ground state by about $\Delta E = 3.7$ K [19,24] (≈ 2.6 cm⁻¹) [25]. These states are well separated (≥ 500 cm⁻¹) from higher-lying spin states [20,21]. The accidentally degenerate $S = 1/2$ doublets are split by gaps of $\Delta_0 = 0.06$ cm⁻¹ (magnetic measurements [22,26]) and $\Delta_0 = 0.28$ cm⁻¹ (inelastic neutron scattering (INS) [27,28]). The microscopic origin of Δ_0 still remains unclear. INS suggested the cause to be distortions from D_3 symmetry [29,30], whereas theory and magnetization pointed to antisymmetric exchange interactions [22,24,26,31,32]. In an applied field of $B_0 = 2.75$ T, the $S = 3/2$ spin state crosses the $S = 1/2$ state. In this region, mixing between the two states might occur whose study might shed light on the origin of Δ_0 . In this paper, we present the results of multifrequency ESR measurements in the proximity of the level crossing. In parallel mode ($B_1 \parallel B_0$) we detected intermultiplet transitions, clear evidence for mixing of spin states. This paves the way to implement qubit interaction switching for QIP. To gain insight into the mechanism of the mixing of spin states in V₁₅ we discuss possible theoretical models, such as antisymmetric exchange [32,33], isosceles distortion, and hyperfine interactions.

II. EXPERIMENTAL SECTION

Single crystals (5 mg) of V₁₅ were prepared and were characterized by published methods [15]. ESR measurements of single V₁₅ crystals were carried out using a homebuilt spectrometer [34]. All measurements were performed at 1.6 K in the frequency range of 4–14 GHz. Frequencies lower than 14 GHz were obtained by inserting dielectrics (Herasil for 7–14 GHz, silicon for 4–7 GHz). No field modulation was employed. ESR spectra were recorded for both parallel $B_1 \parallel B_0$ and perpendicular $B_1 \perp B_0$ magnetic-field directions, where B_1 is the microwave field. Here the sample is placed in the middle of the cylindrical cavity or attached to the top plate of the cavity, respectively [34,35]. The external magnetic field

*slageren@ipc.uni-stuttgart.de

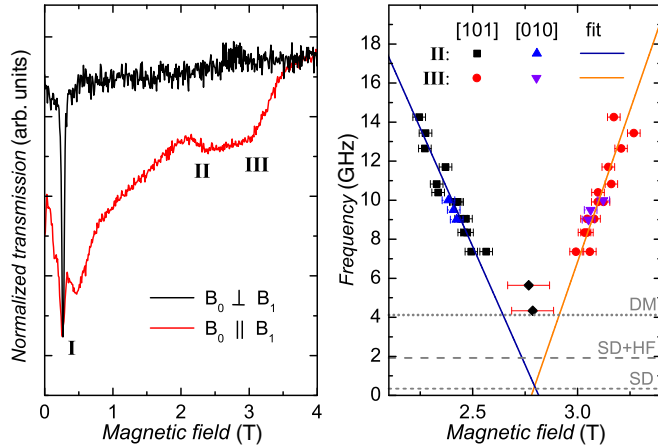


FIG. 1. (Color online) (Left) ESR spectra recorded on the V_{15} cluster at 1.6 K and $\nu = 7.58$ GHz in perpendicular mode and $\nu = 7.36$ GHz in parallel mode. (Right) Frequency versus resonance field from fitting absorption data with linear fits. The horizontal lines indicate the anticrossing gap size, as derived from the different models: Static distortion (SD: short dashed line), including hyperfine interactions (HF: dashed line) and antisymmetric exchange interaction (DM: dots).

B_0 was applied along two orientations [101] and [010] of the unit cell of the single crystal V_{15} (rhombohedral indexing). *Mathematica* [36] was used to calculate the energy-level diagrams and the corresponding eigenvectors to gain insight into the mixing mechanism. Simulations of ESR absorption spectra were carried out with the program EASYPIN [37]. In the case of static distortion, we used as single ion g factors $g_{z,\text{loc}} = 1.95$ and $g_{x,\text{loc}} = g_{y,\text{loc}} = 1.98$ [15,38]. For the hyperfine and antisymmetric exchange models we assumed an isotropic g factor of $g = 1.98$ [32] and an isotropic coupling constant $J = 0.847 \text{ cm}^{-1}$ [26].

III. RESULTS AND DISCUSSION

A. Experimental results

The ESR spectrum recorded at $\nu = 7.58$ GHz in perpendicular mode ($B_1 \perp B_0$) that displays an intensive magnetic resonance peak I at $B_0 = 0.27 \pm 0.05$ T was observed which is attributed to the intramultiplet transitions $M_S = -1/2 \rightarrow M_S = 1/2$ within the ground doublets (Fig. 1, left). In the perpendicular mode, no ESR transitions are observed in the proximity of the level crossing. In contrast, the parallel mode ($B_1 \parallel B_0$) spectrum is profoundly different. At low magnetic fields, a peak is observed at $B_0 \approx 0.3$ T (peak I), which is also attributed to the intramultiplet transitions within the ground doublets. In addition, there is a broad feature overlapping with the resonance line. This was identified as the cavity background signal [34] in empty cavity measurements. Interestingly, at higher fields two additional broad peaks at $B_0 \approx 2.5$ T (peak II) and $B_0 \approx 3.0$ T (peak III) were detected. Their field positions match perfectly with the expected intermultiplet transition energies between $|S = 3/2, M_S = -3/2\rangle$ and $|S = 1/2, M_S = -1/2\rangle$ before and after the level crossing. Thus, the observation of this transition indicates a strong mixing of the different spin states $S = 1/2$ and $S = 3/2$.

This assignment is corroborated by frequency-dependent ESR measurements from 4 to 14 GHz which show two peaks on the right and left sides of the level crossing, whose separation decreases with frequency. Figure 1, right, shows the peak positions as a function of frequency for all measurements from 4 to 14 GHz frequencies and the two orientations [101] and [010] [25]. The clear frequency dependence shows that the observed peaks must be due to transitions of V_{15} . No pronounced orientation dependence was noted. Due to the spectral linewidth it was not possible to distinguish two resonance lines below 7 GHz. However, the total linewidth is smaller than expected for a linear dependence of the resonance field on transition frequency. This suggests that the energy levels may be curved very close to the level crossing, which would indicate the presence of an anticrossing with a gap smaller but not much smaller than 4.33 GHz. The extrapolation of the linear fits (Fig. 1, right) to 0 T yields an offset of $\Delta E = 78$ GHz. This is in perfect agreement with the gap ($\Delta E \approx 3.7 \text{ K} = 77 \text{ GHz}$) between the ground state $S = 1/2$ and the excited state $S = 3/2$.

B. Theoretical considerations

For the theoretical analysis we focus on establishing a minimal model to describe the observed behavior allowing better physical insight into the mechanisms of spin mixing. All calculations were performed in the spin coupled basis $|S_1 S_2 (S_{12}) S_3 M_S\rangle = |(S_{12}) S M_S\rangle$ using irreducible tensor operator (ITO) techniques. S_{12} denotes the intermediate spin quantum number resulting from the coupling of two spins $\hat{S}_{12} = \hat{S}_1 + \hat{S}_2$. The third spin is added according to $\hat{S} = \hat{S}_{12} + \hat{S}_3$ leading to the total spin quantum number S . The simplest Hamiltonian of V_{15} within the three-spin approximation is given by the isotropic Heisenberg-Dirac-Van Vleck exchange interaction and the Zeeman interaction,

$$\hat{H} = 2J(\hat{S}_1 \hat{S}_2 + \hat{S}_2 \hat{S}_3 + \hat{S}_3 \hat{S}_1) + \mu_B \sum_{i=1}^3 \mathbf{B} \bar{g}_i \hat{S}_i. \quad (1)$$

Here \hat{S}_1 , \hat{S}_2 , and \hat{S}_3 denote the single spin operators of the vanadium ions on sites 1, 2, and 3 of the central triangle. J is the antiferromagnetic isotropic exchange interaction parameter, and \bar{g}_i is the single ion g tensor.

1. Static distortion

Considering an isosceles triangle and different isotropic couplings $\Delta = J' - J$ with $\Delta \ll J$ between the vanadium ions, the field-independent Hamiltonian reads

$$\hat{H} = J(\hat{S}^2 - \hat{S}_1^2 - \hat{S}_2^2 - \hat{S}_3^2) + \Delta(\hat{S}_{12}^2 - \hat{S}_1^2 - \hat{S}_2^2). \quad (2)$$

The resulting energy spectrum consists of two doublets $|(0)1/2\rangle$ and $|(1)1/2\rangle$ separated by 2Δ and an excited state $|(1)3/2\rangle$ separated from the ground state by $3J$. We have introduced an isosceles distortion of a triangle which schematically represents the system. Due to the distortion, the vanadium ions are no longer symmetry equivalent. We have assumed that the J values are proportional to the distances between the corners of the triangle ($J, J' \propto r, r'$). Furthermore, we have assumed that the local z axes point from along the line from the center of the triangle through the corner

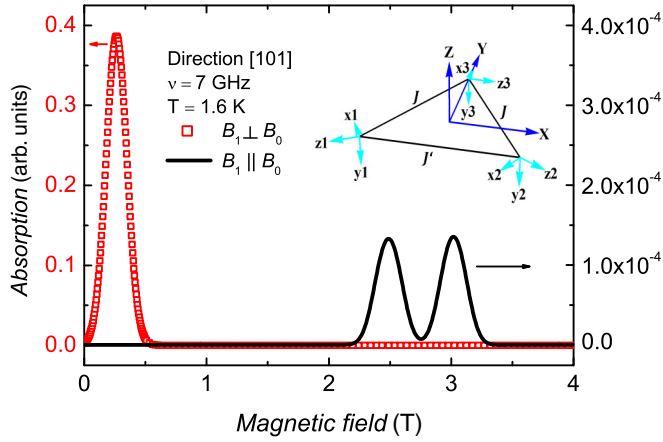


FIG. 2. (Color online) Static distortion. Simulated ESR absorption spectra. Red squares: perpendicular mode ($B_1 \perp B_0$); black solid line: parallel mode ($B_1 \parallel B_0$).

of the triangle, along the V-O bond. Hence the distortion of the triangle introduces a slight rotation of the local g tensors. Rotation matrices were incorporated to interrelate the single ion (nonisotropic) g tensors in the local coordinate frame to the molecular coordinate frame. Subsequently the Hamiltonian of the Zeeman interaction was expressed in terms of ITOs [13,39], and matrix elements were calculated (see Supplemental Material [25]),

$$H_Z^{S'=S} = \mu_B \sum_{q=-1}^1 (-1)^q (\mathbf{B} \bar{g}_{S'}^{[1]})_{-q}^{\parallel} \langle S'_{12} S M' | \hat{S}_q^{[1]} | S_{12} S M \rangle, \quad (3)$$

$$H_Z^{S'=S\pm 1} = \mu_B \sum_{q=-1}^1 \{ (-1)^q [\mathbf{B} (\bar{g}'_{2,\text{loc}} - \bar{g}'_{3,\text{loc}})]_{-q}^{\parallel} \times \langle S'_{12} S' M' | \hat{S}_{12,q}^{[1]} | S_{12} S M \rangle + (-1)^q [\mathbf{B} (\bar{g}'_{1,\text{loc}} - \bar{g}'_{2,\text{loc}})]_{-q}^{\parallel} \times \langle S'_{12} S' M' | \hat{S}_{1,q}^{[1]} | S_{12} S M \rangle \}, \quad (4)$$

with $\bar{g}'_{i,\text{loc}} = \mathbf{R}_i \bar{g}_{i,\text{local}} \mathbf{R}_i^T$.

Hence, it is the different orientations of the local g tensors that lead to nonvanishing matrix elements between different spin multiplets. Figure 2 shows the simulated ESR absorption spectra of V_{15} . The best fits considering all frequencies and orientations were obtained for $J = 0.83$ and $\Delta = 0.05 \text{ cm}^{-1}$ (this corresponds to $\theta = 2^\circ$). Δ was chosen such that the experimental zero-field energy difference between the two $S = 1/2$ states is reproduced. In perpendicular mode, clearly one intensive peak I at low fields is reproduced. For parallel mode, peaks II and III can be simulated. Because they correspond to spin-forbidden transitions, their calculated intensities are much lower. The intensities of both peaks II and III are equal and direction independent. The gap at the level crossings is found to be $\approx 0.3 \text{ GHz}$ (see Fig. 1). In contrast, peak I, which corresponds to an intramultiplet transition between $|0\rangle 1/2$ and $|1\rangle 1/2$ was not reproduced in parallel mode. There is no transition matrix element within the Hamilton matrix for these states (see Supplemental Material [25]). Hence a

static distortion of the triangle alone cannot reproduce the experimental data.

2. Hyperfine interaction

The mixing of different spin states can also be caused by hyperfine interaction. The nuclear spin of a vanadium ion is $I = 7/2$. The hyperfine term of the Hamiltonian for an equilateral triangle (isotropic g factor) and isotropic hyperfine coupling constant A is given by

$$\hat{H} = A \sum_{i=1}^3 \hat{\mathbf{I}}_i \hat{\mathbf{S}}_i. \quad (5)$$

In this case the local coordinate systems coincide with the molecular one, maintaining the overall D_3 symmetry. Again ITOs are used to express the Hamiltonian and calculate the matrix elements,

$$H_{\text{hyp}}^{S'=S} = A \sum_{q=-1}^1 (-1)^q \langle I'_{12} I' M'_I | \hat{I}_{-q}^{S,[1]} | I_{12} I M_I \rangle \times \langle S'_{12} S M' | \hat{S}_q^{[1]} | S_{12} S M \rangle, \quad (6)$$

$$H_{\text{hyp}}^{S'=S\pm 1} = A \sum_{q=-1}^1 [(-1)^q \langle I'_{12} I' M'_I | \hat{I}_{2,-q}^{[1]} - \hat{I}_{3,-q}^{[1]} | I_{12} I M_I \rangle \times \langle S'_{12} S' M' | \hat{S}_{12,q}^{[1]} | S_{12} S M \rangle + (-1)^q \langle I'_{12} I' M'_I | \hat{I}_{1,-q}^{[1]} - \hat{I}_{2,-q}^{[1]} | I_{12} I M_I \rangle \times \langle S'_{12} S' M' | \hat{S}_{1,q}^{[1]} | S_{12} S M \rangle]. \quad (7)$$

The nuclear spin operator $\hat{\mathbf{I}}_i$ is an operator acting on the coupled nuclear spin basis $|I_1 I_2 (I_{12}) I_3 I M_I\rangle = |(I_{12}) I M_I\rangle$. Not all nuclear transition matrix elements vanish because the single nuclear spin operators are not equivalent within some subspaces (similar to the different local g tensors in the isosceles model). Therefore, matrix elements between different spin multiplets exist, and a mixing of spin states is possible. The simulations were performed with an isotropic hyperfine interaction constant $A_I^S = 10 \text{ mK} \approx 0.007 \text{ cm}^{-1}$ [40,41] (Fig. 3). Again, a single intensive peak I is reproduced for perpendicular mode. For $B_1 \parallel B_0$ all three peaks I, II, and III are simulated. Peak I corresponds to an intermediate-spin multiplet transition. The positions and intensities of the peaks are direction independent and in good agreement with the measured data. Nevertheless, the hyperfine coupling constant A is on the order of ten times too small to describe the correct magnitude of Δ_0 [42]. Hence, hyperfine interaction alone cannot reproduce the characteristics of V_{15} . However, a combination of static distortion with hyperfine interaction can reproduce the experimental data. In this case the gap of the anticrossing is on the order of $\approx 1 \text{ GHz}$ (Fig. 1).

3. Antisymmetric exchange interaction

Because of the long ongoing debate about the correct model to describe the V_{15} molecule, we also attempted to simulate our data by incorporating the antisymmetric exchange or Dzhaldoshinskii-Moriya (DM) interaction [43,44]. The DM

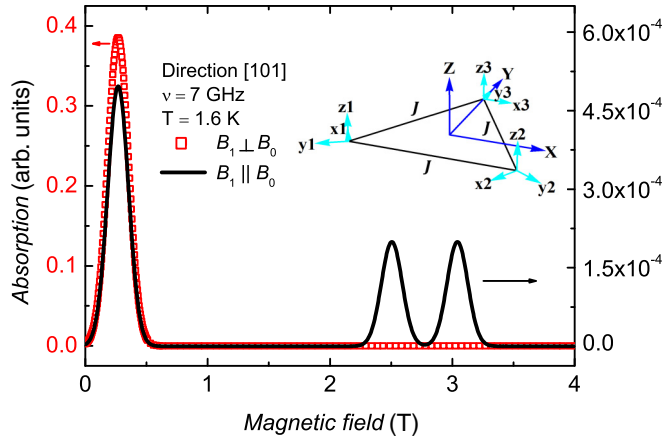


FIG. 3. (Color online) Hyperfine interaction. Simulated ESR absorption spectra. Red squares: perpendicular mode ($B_1 \perp B_0$); black solid line: parallel mode ($B_1 \parallel B_0$).

Hamiltonian of the V_{15} cluster reads

$$\hat{H} = \mathbf{D}_{12}[\hat{\mathbf{S}}_1 \times \hat{\mathbf{S}}_2] + \mathbf{D}_{23}[\hat{\mathbf{S}}_2 \times \hat{\mathbf{S}}_3] + \mathbf{D}_{31}[\hat{\mathbf{S}}_3 \times \hat{\mathbf{S}}_1]. \quad (8)$$

\mathbf{D}_{ij} is the vector of the antisymmetric exchange interaction between two vanadium ions. Taking into account the actual D_3 symmetry of V_{15} , vector \mathbf{D}_{ij} is perpendicular to the C_2 axis according to Moriya's conditions [44]. Thus, the DM vector is given by two components, the normal (normal to the plane of the triangle) component $D_n (=D_{12}^z = D_{23}^z = D_{31}^z)$ and the in-plane component $D_\perp (=D_{12}^x = D_{23}^x = D_{31}^x)$. Tsukerblat *et al.* [31–33] investigated the role of DM interactions within V_{15} in detail. The normal component D_n is a first-order effect and causes the gap ($\sqrt{3}D_n - D_\perp^2/8J$) between the accidentally degenerate ground states. The DM interaction depends on the orientation of the magnetic field. In the proximity of the level crossing, the in-plane component of the DM interaction was shown to be a first-order perturbation resulting in the mixing of different total spin states [31]. The gap at the crossing point is found to be $3D_\perp/2$, independent of D_n . Our measurements showed that the size of this gap is maximum 4.33 GHz, thus $D_\perp \leq 0.09 \text{ cm}^{-1}$ (respectively, $D_\perp \leq 0.11J$). Compared to the value of Tarantul *et al.* [45], $D_\perp \approx 0.238 \text{ cm}^{-1}$ from fitting magnetic data, our in-plane component is smaller. Figure 4 shows the simulated ESR absorption spectra of the V_{15} system. The spectra are similar for both orientations. The best simulations were performed using $D_n = \pm 0.06J$. For D_\perp we assumed the upper limit. Thus, the gap of the ground state is 0.09 cm^{-1} (see Fig. 1), which is in good agreement with the value from magnetic measurements. Peak I is well reproduced for $B_1 \perp B_0$ showing no sign dependence of the normal or in-plane component. For parallel mode, all three peaks I, II, and III could be simulated. The intensities slightly depend on the sign of D_n respective to that of D_\perp .

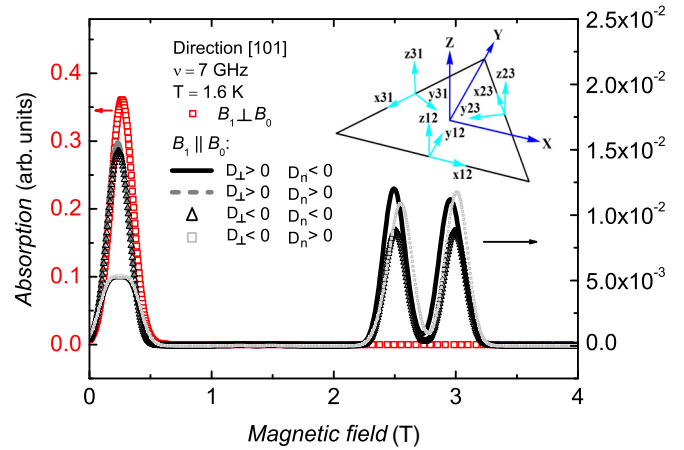


FIG. 4. (Color online) DM interaction. Simulated ESR absorption spectra. Red squares: perpendicular mode ($B_1 \perp B_0$); black solid line: parallel mode ($B_1 \parallel B_0$) for $D_n < 0$ and $D_\perp > 0$; gray dotted line: $D_n > 0$ and $D_\perp > 0$; black triangles: $D_n < 0$ and $D_\perp < 0$, and gray squares: $D_n > 0$ and $D_\perp < 0$.

The DM exchange interaction can also reproduce our experimental data. The orientation dependence in the case of the DM interaction model is larger than for the combination of hyperfine interactions and isosceles distortion. However, the effect is too small to be detectable in our measurements.

IV. CONCLUSION

In V_{15} spin-forbidden ESR transitions between the $S = 1/2$ and the $S = 3/2$ states were detected in the proximity of the level crossing at 2.75 T for a range of different frequencies. This is unambiguous evidence for a mixing of spin states. This opens the way to switch qubit interactions for quantum computation applications. Theoretical considerations and simulations of the absorption spectra indicate that two models: (1) A combination of hyperfine interaction and static distortion of the triangle or (2) antisymmetric exchange interaction can reproduce the experimental data. If one interprets the field positions of the two lowest-frequency points in Fig. 1 (right) as being indicative of curvature of the field-frequency plot, this would indicate proximity to an anticrossing. In that case the antisymmetric exchange interaction scenario becomes the most plausible, given that the anticrossing gap is calculated to be much smaller for the other two scenarios for reasonable parameter values (Fig. 1).

ACKNOWLEDGMENTS

We gratefully acknowledge financial support from DFG and IMPRS-AM (C.S.). We also thank Professor M. Dressel (University of Stuttgart) for useful discussions as well as Professor H. Schweizer for lending the network analyzer used in this paper.

[1] S. Carretta, P. Santini, G. Amoretti, F. Troiani, and M. Affronte, *Phys. Rev. B* **76**, 024408 (2007).

[2] P. Santini, S. Carretta, F. Troiani, and G. Amoretti, *Phys. Rev. Lett.* **107**, 230502 (2011).

- [3] F. Troiani and M. Affronte, *Chem. Soc. Rev.* **40**, 3119 (2011).
- [4] J. Slageren, *Top. Curr. Chem.* **321**, 199 (2012).
- [5] A. Ardavan, O. Rival, J. J. L. Morton, S. J. Blundell, A. M. Tyryshkin, G. A. Timco, and R. E. P. Winpenny, *Phys. Rev. Lett.* **98**, 057201 (2007).
- [6] S. Bertaina, S. Gambarelli, T. Mitra, B. Tsukerblat, A. Müller, and B. Barbara, *Nature (London)* **453**, 203 (2008).
- [7] K.-Y. Choi, Y. H. Matsuda, H. Nojiri, U. Kortz, F. Hussain, A. C. Stowe, C. Ramsey, and N. S. Dalal, *Phys. Rev. Lett.* **96**, 107202 (2006).
- [8] M. Trif, F. Troiani, D. Stepanenko, and D. Loss, *Phys. Rev. Lett.* **101**, 217201 (2008).
- [9] P. Lutz, R. Marx, D. Dengler, A. Kromer, and J. van Slageren, *Mol. Phys.* **111**, 2897 (2013).
- [10] G. Mitrikas, Y. Sanakis, C. P. Raptopoulou, G. Kordas, and G. Papavassiliou, *Phys. Chem. Chem. Phys.* **10**, 743 (2008).
- [11] Y. Sanakis, A. K. Boudalis, and J.-P. Tuchagues, *C. R. Chim.* **10**, 116 (2007).
- [12] S. Datta, O. Waldmann, A. D. Kent, V. A. Milway, L. K. Thompson, and S. Hill, *Phys. Rev. B* **76**, 052407 (2007).
- [13] R. Boča, *Theoretical Foundations of Molecular Magnetism, Current Methods in Inorganic Chemistry Vol. 1* (Elsevier Science, Lausanne, Switzerland, 1999).
- [14] J. C. Goodwin, R. Sessoli, D. Gatteschi, W. Wernsdorfer, A. K. Powell, and S. L. Heath, *J. Chem. Soc., Dalton Trans.*, 1835 (2000).
- [15] A. Müller and J. Döring, *Angew. Chem., Int. Ed. Engl.* **27**, 1721 (1988).
- [16] A. Tarantul and B. Tsukerblat, *The Nanoscopic V_{15} Cluster: A Unique Magnetic Polyoxometalate* (World Scientific, Singapore, 2011), Chap. 3, pp. 109–179.
- [17] S. Bertaina, S. Gambarelli, T. Mitra, B. Tsukerblat, A. Müller, and B. Barbara, *Nature (London)* **466**, 1006 (2010).
- [18] J. Yang, Y. Wang, Z. Wang, X. Rong, C.-K. Duan, J.-H. Su, and J. Du, *Phys. Rev. Lett.* **108**, 230501 (2012).
- [19] D. Gatteschi, L. Pardi, A. L. Barra, A. Müller, and J. Döring, *Nature (London)* **354**, 463 (1991).
- [20] A. L. Barra, D. Gatteschi, L. Pardi, A. Müller, and J. Döring, *J. Am. Chem. Soc.* **114**, 8509 (1992).
- [21] D. Gatteschi, L. Pardi, A. Barra, and A. Müller, *Mol. Eng.* **3**, 157 (1993).
- [22] I. Chiorescu, W. Wernsdorfer, A. Müller, S. Miyashita, and B. Barbara, *Phys. Rev. B* **67**, 020402 (2003).
- [23] H. De Raedt, S. Miyashita, and K. Michielsen, *Phys. Status Solidi* **241**, 1180 (2004).
- [24] H. De Raedt, S. Miyashita, K. Michielsen, and M. Machida, *Phys. Rev. B* **70**, 064401 (2004).
- [25] See Supplemental Material at <http://link.aps.org/supplemental/10.1103/PhysRevB.90.144405> for experimental data, calculation of the matrix elements and further simulations.
- [26] I. Chiorescu, W. Wernsdorfer, A. Müller, H. Bögge, and B. Barbara, *J. Magn. Magn. Mater.* **221**, 103 (2000).
- [27] G. Chaboussant, R. Basler, A. Sieber, S. T. Ochsenbein, A. Desmedt, R. E. Lechner, M. T. F. Telling, P. Kögerler, A. Müller, and H.-U. Güdel, *Europhys. Lett.* **59**, 291 (2002).
- [28] G. Chaboussant, R. Basler, A. Sieber, S. Ochsenbein, and H.-U. Güdel, *Physica B* **350**, E51 (2004).
- [29] G. Chaboussant, S. T. Ochsenbein, A. Sieber, H.-U. Güdel, H. Mutka, A. Müller, and B. Barbara, *Europhys. Lett.* **66**, 423 (2004).
- [30] M. Baker and H. Mutka, *Eur. Phys. J.: Spec. Top.* **213**, 53 (2012).
- [31] B. Tsukerblat, A. Tarantul, and A. Müller, *Phys. Lett. A* **353**, 48 (2006).
- [32] B. Tsukerblat, A. Tarantul, and A. Müller, *J. Chem. Phys.* **125**, 054714 (2006).
- [33] B. Tsukerblat, A. Tarantul, and A. Müller, *Chem. J. Moldova* **2**, 17 (2007).
- [34] C. Schlegel, M. Dressel, and J. van Slageren, *Rev. Sci. Instrum.* **81**, 093901 (2010).
- [35] C. Schlegel, Ph.D. thesis, Universität Stuttgart, 2009.
- [36] Wolfram Research, Inc., *Mathematica* (2010), Version 8.0, Champaign, IL.
- [37] S. Stoll and A. Schweiger, *J. Magn. Reson.* **178**, 42 (2006).
- [38] S. Vongtragool, B. Gorshunov, A. A. Mukhin, J. van Slageren, M. Dressel, and A. Müller, *Phys. Chem. Chem. Phys.* **5**, 2778 (2003).
- [39] D. A. Varshalovich, A. N. Moskalev, and V. K. Khersonskii, *Quantum Theory of Angular Momentum* (World Scientific, Singapore, 1988).
- [40] I. Chiorescu, W. Wernsdorfer, A. Müller, H. Bögge, and B. Barbara, *Phys. Rev. Lett.* **84**, 3454 (2000).
- [41] A. Weiss, *Ber. Bunsenges. Phys. Chem.* **81**, 779 (1977).
- [42] S. Miyashita, H. D. Raedt, and K. Michielsen, *Prog. Theor. Phys.* **110**, 889 (2003).
- [43] I. Dzyaloshinsky, *J. Phys. Chem. Solids* **4**, 241 (1958).
- [44] T. Moriya, *Phys. Rev.* **120**, 91 (1960).
- [45] A. Tarantul, B. Tsukerblat, and A. Müller, *Chem. Phys. Lett.* **428**, 361 (2006).